Available online at www.pelagiaresearchlibrary.com

Pelagia Research Library

Advances in Applied Science Research, 2011, 2 (3):265-279

ISSN: 0976-8610
CODEN (USA): AASRFC

The Influence of Wall Properties on MHD Peristaltic transport of Dusty Fluid

V. P. Rathod and Pallavi kulkarni

Department of Studies and Research in Mathematics, Gulbarga University, Gulbarga, Karnataka, India

---

ABSTRACT

The interaction between peristaltic transport of a dusty fluid (Saffman's model) in a two-dimensional uniform channel and the elasticity of the channel's flexible walls was studied under long wavelength approximation and uniform magnetic field. Perturbation solutions were obtained for the stream functions of both the fluid particles and solid particles, in terms of the wall slope parameter. The expressions for average velocity of the fluid particles and solid particles, and average fluid flow rate were derived.

Key words: Peristaltic transport, Wall properties, Dust particles, Magnetic field.

INTRODUCTION

Peristaltic pumping is the transport of a fluid via traveling waves imposed on the walls of the tube or channel. This is known to be a major mechanism in biological systems, including urine transport from the kidneys to the bladder through the ureter. The industrial use of Peristaltic pumping in roller/ finger pumps is well known. Engineers to pump corrosive materials and fluids that must be kept away from pumping machinery have adopted this principle. In particular, the peristaltic transport of toxic liquid is used by the nuclear industry so as not to contaminate the environment. Peristaltic pumping is used in biomedical devices such as the heart-lung machine to pump blood. It is also speculated that peristalsis may be involved in the translocation of water in tall trees. The translocation of water involves its motion through the porous matrix of the trees.

Many of these studies explained the basic fluid mechanical aspects of peristalsis and two important phenomena trapping and reflux. Reflux refers to the net retrograde motion of some part of a fluid in a direction opposite that of wave propagation on the wall and trapping is the development and transport of an internally circulating bolus of fluid (Shapiro [1]). Fung and Yih [2] observed that pumping against a positive pressure gradient than a critical value results in a backward flow in the central region of the stream. Jaffrin and Shapiro [3] provide an elaborate review of the curlier literature regarding peristalsis. As the behavior of most physiological fluids is known to be non-Newtonian, attempts have been made to analyze the peristaltic transport of non-Newtonian fluids. Several researchers (Picologlou et al [4]; Srivatsava [5]; Misery et al [6];

Srinivacharya et al [7]) that described the non-Newtonian behavior of fluids as power law, couple stress, micro polar, and generalized Newtonian fluid models, respectively investigated peristaltic transport of blood in small vessels.

Saffman's [8] dusty fluid model serves as a good model for describing blood as a binary system. Kaimal [9] studied peristaltic transport of a solid- fluid mixture at a low Reynolds number under long wavelength approximation. Radhakrishnamacharya [10] studied the pulsatile flow of a fluid containing small solid particles through a two-dimensional constricted channel.

Mitra and Prasad [11] studied peristaltic transport of a Newtonian viscous fluid in a two-dimensional uniform channel while considering the elasticity of the wall. They reported that flow reversal occurs at the center of the channel if the walls of the channel are elastic and that the position may shift to the boundaries if the viscous damping forces are considered. Srinivasalu and Radhakrishnacharya [12] studied peristaltic transport in a non- uniform channel with elastic effects. Srinivasacharya et al. [13] studied the effect of wall properties on peristaltic transport of a dusty fluid. Rathod and Asha [14] studied the peristaltic transport of a couple stress fluid in uniform and non-uniform annulus moving with a constant velocity. Rathod and Mahadev [15] studied the Effect magnetic field on Ureteral peristalsis in cylindrical tube. Study of this interaction under different conditions may lead to a better understanding of the role of peristalsis in the transport of physiological fluids.

The present research aimed is to study the effects of channel wall properties on peristaltic transport of a Hydro magnetic dusty fluid (Saffman's model) through a two-dimensional channel. The expressions for average velocity of the fluid particles and solid particles, and average fluid flow rate were derived. The effects of various elastic parameters and mass concentration of dust particles on the streamline pattern and average fluid flow rate were studied.

Formulation of the problem

Consider the laminar flow of an incompressible fluid that contains small solid particles, whose number density (N) (assumed to be a constant N_0) is large enough to define average properties of the dust particles at a point through a symmetrical two-dimensional channel. Peristaltic waves of long wavelength are assumed to travel along the walls of the channel. The geometry of the wall surface is described by

$$\eta = d + a\sin\left(\frac{2\pi}{\lambda}(x-ct)\right) \tag{1}$$

Where d is the width of the channel, a is the amplitude of the wave, λ is the wave length and t is time (Figure1).

The equations of motion of a viscous incompressible fluid with uniform distribution of solid particles are given by Saffman (1962). The flow of the fluid is governed by the continuity and momentum equation.

$$\nabla . V = 0 \tag{2}$$

$$\frac{\partial V}{\partial t} + (V.\nabla)V = -\frac{1}{\rho}\nabla p + \upsilon\nabla^2 V + \frac{KN_0}{\rho}(V_s - V) - \sigma\frac{B_0^2}{\rho}V \tag{3}$$

The motion of the dust particles is governed by Newton's second law is

$$\frac{\partial V_s}{\partial t} + (V_s.\nabla)V_s = \frac{K}{m}(V - V_s) \tag{4}$$

And the continuity equation

$$\nabla.V_s = 0 \tag{5}$$

Where $V_s = [u_s, v_s]$ is the velocity of solid particles and m is the mass of the solid particles.

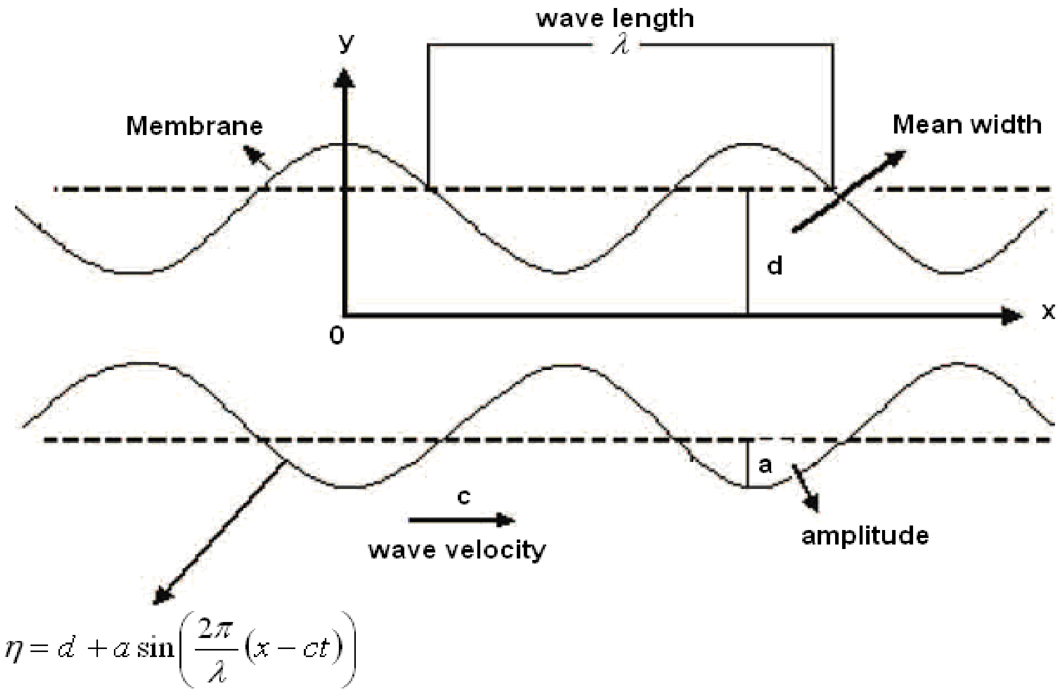

Figure1. Geometry of two-dimensional peristaltic motion of channel walls.

Where $V = [u, v]$ is the velocity of the fluid particles, p is the fluid pressure, σ electrical conductivity of the fluid, B_0 is the applied magnetic field, ρ is the density of the fluid, υ is the kinematic coefficient of the viscosity of fluid, and K is the resistance coefficient for the dust particles-a constant. The first two terms on the right side of Eq. (3) are, respectively, the pressure gradient and viscosity terms. The last term represents the force due to the relative motion between the fluid and solid particles. It is assumed that the Reynolds number of the relative velocity is small. In such a case, the force between the solid and fluid is proportional to the relative velocity.

The governing equation of motion of the flexible wall may be expressed as

$$L(\eta) = p - p_0 \tag{6}$$

Where L is an operator that is used to represent the motion of the stretched membrane with damping forces such that

$$L = -T\frac{\partial^2}{\partial x^2} + m'\frac{\partial^2}{\partial t^2} + C\frac{\partial}{\partial t} \tag{7}$$

Here, T is the tension in the membrane, m' is mass per unit area, C is the coefficient of viscous damping forces, and p_0 is the pressure on the outside of the wall due to tension in the muscles. This tension may be due to the constitutive relations of the muscles when the displacements are known. Certain terms may be added to Eq. (7) to account for spring foundations, but they do not change the mathematical nature of the problem; therefore, to keep the analysis simple they are not considered herein (Mitra and Prasad, 1973).

It is assumed that p_0=0 and the walls of the channel are inextensible, so that only their lateral motion takes place and the horizontal displacement of the wall is zero. Thus, the no-slip boundary condition for the velocities is

$$u = 0, u_s = 0 \text{ At } y = \pm\eta \tag{8}$$

Continuity of stresses requires that at the interfaces of the walls and fluid p must be the same as that which acts on the fluid at $y = \pm\eta$ .the use of the x-momentum equation yields

$$\frac{\partial}{\partial x}(L(\eta)) = \frac{\partial p}{\partial x} = \rho \upsilon\left[\frac{\partial^2 u}{\partial x^2} + \frac{\partial^2 u}{\partial y^2}\right] - \rho\left[\frac{\partial u}{\partial x} + u\frac{\partial u}{\partial y} + v\frac{\partial u}{\partial y}\right] + \frac{KN_0}{\rho}(u_s - u) - \sigma\frac{B_0^2}{\rho}u$$

at $y = \pm\eta$ (9)

Introducing the steam functions ψ and ϕ such that

$$u = \frac{\partial\psi}{\partial y}, v = -\frac{\partial\psi}{\partial x}, u_s = \frac{\partial\phi}{\partial y}, v_s = \frac{\partial\phi}{\partial x} \tag{10}$$

and following non-dimensional variables

$$x' = x/\lambda, y' = y/d, \eta' = \eta/d, t' = (vt)/(\lambda d), \psi' = \psi/v, \phi' = \phi/(Kd^2/m) \tag{11}$$

into Equations. (2)- (5), we obtain the following equations (after dropping primes and eliminating the pressure term)

$$\delta\left[\frac{\partial}{\partial t}(\nabla_1^2\psi) + \frac{\partial\psi}{\partial y}\frac{\partial}{\partial x}(\nabla_1^2\psi) - \frac{\partial\psi}{\partial x}\frac{\partial}{\partial y}(\nabla_1^2\psi)\right] = \nabla_1^4\psi + P\left[\frac{1}{R}\nabla_1^2\phi - \nabla_1^2\psi\right] - M^2(\nabla_1^2\psi) \tag{12}$$

$$\delta\left[R\frac{\partial}{\partial t}(\nabla_1^2\phi) + \frac{\partial\phi}{\partial y}\frac{\partial}{\partial x}(\nabla_1^2\phi) - \frac{\partial\phi}{\partial x}\frac{\partial}{\partial y}(\nabla_1^2\phi)\right] = R\nabla_1^2\psi - \nabla_1^2\phi \tag{13}$$

Where $\nabla_1^2 = \left(\delta^2 \frac{\partial^2}{\partial x^2} + \frac{\partial}{\partial y^2}\right), \varepsilon = a/d, \delta = d/\lambda$ are geometric parameters and

$R = \frac{\upsilon m}{Kd^2}$ and $P = \frac{KN_0 d^2}{\rho\upsilon}$ are non-dimensional parameters.

And $M^2 = B_0 d\sqrt{\frac{\sigma}{\mu}}$ is the Hartman number.

The boundary conditions in non-dimensional form now become

$$\frac{\partial\psi}{\partial y} = \frac{\partial\phi}{\partial y} = 0 \qquad \text{at} \qquad y = \pm\eta = \pm(1+\varepsilon\sin 2\pi(x-t)) \tag{14}$$

$$\nabla_1^2 \frac{\partial\psi}{\partial y} - \delta\left[\frac{\partial}{\partial t}\frac{\partial\psi}{\partial y} + \frac{\partial\psi}{\partial y}\frac{\partial}{\partial x}\frac{\partial\psi}{\partial y} - \frac{\partial}{\partial x}\frac{\partial}{\partial y}\frac{\partial\psi}{\partial y}\right] + P\left(\frac{1}{R}\frac{\partial\phi}{\partial y} - \frac{\partial\psi}{\partial y}\right) - M^2\frac{\partial\psi}{\partial y} =$$
$$\left(E_1\frac{\partial^3}{\partial x^3} + E_2\frac{\partial^3}{\partial x\partial t^2} + E_3\frac{\partial^2}{\partial x\partial t}\right)\eta$$
$$\text{at } y = \pm\eta = \pm(1+\varepsilon\sin 2\pi(x-t)) \tag{15}$$

Where $E_1 = \frac{Td^4}{\upsilon\rho}$, membrane tension parameter,

$E_2 = \frac{m' d^2}{\lambda^3\rho}$, mass characterizing parameter, and

$E_3 = \frac{cd^3}{\lambda^2\upsilon\rho}$, damping parameter.

Method of Solution

Assuming the parameters δ is very small, the stream functions ψ and ϕ may be expanded in power series of δ as

$$\begin{aligned} \psi &= \psi_0 + \delta\psi_1 + \delta^2\psi_2 + \ldots \\ \phi &= \phi_0 + \delta\phi_1 + \delta^2\phi_2 + \ldots \end{aligned} \tag{16}$$

Substituting Equation (16) in Eqs. (12) - (15) and collecting the coefficients of various powers of δ on both sides, we obtain the following sets of coupled linear differential equations for ψ_0, ϕ_0 and ψ_1, ϕ_1, ϕ_1:

Zeroth order in δ

$$\frac{\partial^4\psi_0}{\partial y^4} + P\left(\frac{1}{R}\frac{\partial^2\phi_0}{\partial y^2} - \frac{\partial^2\psi_0}{\partial y^2}\right) - M^2\frac{\partial^2\psi_0}{\partial y^2} = 0 \tag{17}$$

$$R\frac{\partial^2\phi_0}{\partial y^2}-\frac{\partial^2\psi_0}{\partial y^2}=0 \tag{18}$$

And the corresponding boundary conditions at $y=\pm\eta$ are

$$\frac{\partial\phi_0}{\partial y}=\frac{\partial\psi_0}{\partial y}=0 \tag{19}$$

$$\frac{\partial^3\psi_0}{\partial y^3}+P\left(\frac{1}{R}\frac{\partial\phi_0}{\partial y}-\frac{\partial\psi_0}{\partial y}\right)-M^2\frac{\partial\psi_0}{\partial y}=\left(E_1\frac{\partial^3}{\partial x^3}+E_2\frac{\partial^3}{\partial x\partial t^2}+E_3\frac{\partial^2}{\partial x\partial t}\right)\eta \tag{20}$$

First order in δ

$$\frac{\partial^4\psi_1}{\partial y^4}+P\left(\frac{1}{R}\frac{\partial^2\phi_1}{\partial y^2}-\frac{\partial^2\psi_1}{\partial y^2}\right)-M^2\frac{\partial^2\psi_1}{\partial y^2}=\frac{\partial^3\psi_0}{\partial t\partial y^2}+\frac{\partial\psi_0}{\partial y}\frac{\partial^3\psi_0}{\partial x\partial y^2}-\frac{\partial\psi_0}{\partial x}\frac{\partial^3\psi_0}{\partial y^3} \tag{21}$$

$$R\frac{\partial^2\psi_1}{\partial y^2}-\frac{\partial^2\phi_1}{\partial y^2}=R\frac{\partial^3\phi_0}{\partial t\partial y^2}+\frac{\partial\phi_0}{\partial y}\frac{\partial^3\phi_0}{\partial x\partial y^2}-\frac{\partial\phi_0}{\partial x}\frac{\partial^3\phi_0}{\partial y^3} \tag{22}$$

and the corresponding boundary conditions at $y=\pm\eta$ are

$$\frac{\partial\phi_1}{\partial y}=\frac{\partial\psi_1}{\partial y}=0 \tag{23}$$

$$\frac{\partial^3\psi_1}{\partial y^3}+P\left(\frac{1}{R}\frac{\partial\phi_1}{\partial y}-\frac{\partial\psi_1}{\partial y}\right)-M^2\frac{\partial\psi_1}{\partial y}=\frac{\partial^2\psi_0}{\partial t\partial y}+\frac{\partial\psi_0}{\partial y}\frac{\partial^2\psi_0}{\partial x\partial y}-\frac{\partial\psi_0}{\partial x}\frac{\partial^2\psi_0}{\partial y^2} \tag{24}$$

The solutions of Eq. (17) and (18), subject to the boundary conditions (19) and (20), are

$$\psi_0=\frac{A_1\left(y^3-3\eta^2y\right)}{1-\frac{M^2}{2}\left(y^2-2\eta y\right)} \tag{25}$$

$$\phi_0=\frac{A_1R\left(y^3-3\eta^2y\right)}{1-\frac{M^2}{2}\left(y^2-2\eta y\right)} \tag{26}$$

Where $A_1=-\frac{\varepsilon}{6}\left[(2\pi)^3(E_1+E_2)Cos2\pi(x-t)-E_3(2\pi)^2Sin2\pi(x-t)\right]$

Similarly, the solutions of Eq. (21) and (22) subject to the boundary conditions (23) and (24) are

$$\psi_1=\left[\frac{B_1y^7}{840}+\frac{B_2y^5}{120}+\frac{B_3y^3}{6}+B_4y\right]\Big/1-\frac{M^2}{2}\left(y^2-2\eta y\right) \tag{27}$$

$$\phi_1 = \frac{R\left(\frac{B_1 y^7}{840}+\frac{B_2 y^5}{120}+\frac{B_3 y^3}{6}+B_4 y\right)}{\left(1-\frac{M^2}{2}\left(y^2-2\eta y\right)\right)^2} - \frac{6R^2\left(\frac{D_1 y^5}{20}+\frac{D_2 y^3}{6}+D_3 y\right)}{\left(1-\frac{M^2}{2}\left(y^2-2\eta y\right)\right)} \tag{28}$$

Where

$$B_1 = 12(1+S)A_1(\partial A_1/\partial x)$$

$$B_2 = 6(1+S)\left[6A_1^2\eta(\partial\eta/\partial x)+(\partial A_1/\partial t)\right]$$

$$B_3 = 12A_1(\partial A_1/\partial x)\eta^4 + 36A_1^2\eta^3(\partial\eta/\partial x) - 6A_1\eta(\partial\eta/\partial t) - \frac{B_1}{4}\eta^4 - \frac{B_2}{2}\eta^2$$

$$B_4 = -\left(\frac{B_1}{120}\eta^6+\frac{B_2}{24}\eta^4+\frac{B_3}{2}\eta^2\right)$$

$$D_1 = B_1/\left[6(1+S)\right]$$

$$D_2 = B_2/\left[6(1+S)\right]$$

$$D_1 = 6R^2\left(\frac{D_1}{4}\eta^4+\frac{D_2}{2}\eta^2\right)$$

$S = \frac{N_0 m}{\rho}$, mass concentration of dust particles.

Average axial velocities of the fluid particle ($\bar{u}$) and the solid particle ($\bar{u}_s$) (up to first order) over one period of motion are given by

$$\bar{u} = \int_0^1 u\,dt \tag{29}$$

$$\bar{u}_s = \int_0^1 u_s\,dt \tag{30}$$

Where

$$u = \frac{3A_1\left(y^2-\eta^2\right)X + M^2(y-\eta)A_1\left(y^3-3\eta^2 y\right)}{X^2} + \frac{\delta\left\{X^2\left[\frac{B_1 y^6}{120}+\frac{B_2 y^4}{24}+\frac{B_3 y^2}{2}+B_4\right]+2M^2(y-\eta)X\left[\frac{B_1 y^7}{840}+\frac{B_2 y^5}{120}+\frac{B_3 y^3}{6}+B_4 y\right]\right\}}{X^4} \tag{31}$$

$$u_s = \frac{3RA_1\left(y^2-\eta^2\right)X + M^2\left(y-\eta\right)A_1R\left(y^3-3\eta^2 y\right)}{X^2}$$
$$+\frac{\delta\left\{RX^2\left[\frac{B_1y^6}{120}+\frac{B_2y^4}{24}+\frac{B_3y^2}{2}+B_4\right]+2M^2R\left(y-\eta\right)X\left[\frac{B_1y^7}{840}+\frac{B_2y^5}{120}+\frac{B_3y^3}{6}+B_4y\right]\right\}}{X^4}$$
$$+\frac{6R^2\delta\left\{X\left(\frac{D_1y^4}{4}+\frac{D_2y^2}{2}+D_3\right)+M^2\left(\frac{D_1y^5}{20}+\frac{D_2y^3}{6}+D_3y\right)\right\}}{X^2} \qquad (32)$$

Where $X = \left(1-\frac{M^2}{2}\left(y^2-2\eta y\right)\right)$

The fluid flow rate (Q) defined by

$$Q = \int_0^{\eta} u\,dy \qquad (33)$$

can be obtained using Eq. (31) as

$$Q = \frac{-2A_1\eta^3}{\left(1+\frac{M^2}{2}\eta^2\right)} + \frac{\delta\left[\frac{B_1\eta^7}{840}+\frac{B_2\eta^5}{120}+\frac{B_3\eta^3}{6}+B_4\eta\right]}{\left(1+\frac{M^2}{2}\eta^2\right)^2} \qquad (34)$$

The time average flow rate over a period defined by

$$\bar{Q} = \int_0^1 Q\,dt \qquad (35)$$

can be obtained using Eq. (34).

RESULTS AND DISCUSSION

To explicitly see the effects of various parameters on these flow variables, these quantities were numerically evaluated and the results are graphically presented in Figure 2-8. The rigid nature of the wall is represented by the parameter E_1, which depends on the wall tension and E_2 represents the stiffness property of the wall. The parameter E_3 represents the dissipative feature of the wall. The choice E_3=0 implies that the wall moves up and down, with no damping force on it and, therefore, indicates the case of elastic walls.

The effect of the rigid nature of the walls on the streamline patterns for the elastic walls (E_3=0) is shown in the Figure 2a and 2b. It can seen from the figure that the streamline got closer as the tension parameter (E_1) increased and the phenomenon of trapping was observed. It is significant to note that the trapping phenomenon became predominant and the area of the trapped bolus increased as the tension parameter increased. The effect of the dissipative feature of the walls on the streamline are given in Figure 2c and 2d. Figure 2c and 2d shows that, as the dissipative feature of the wall increased, change in the character of the streamlines for fixed values of E_1 was not significant. Though trapping was observed and was predominant, it can be seen that as damping increased the area of the trapped bolus in some regions decreased.

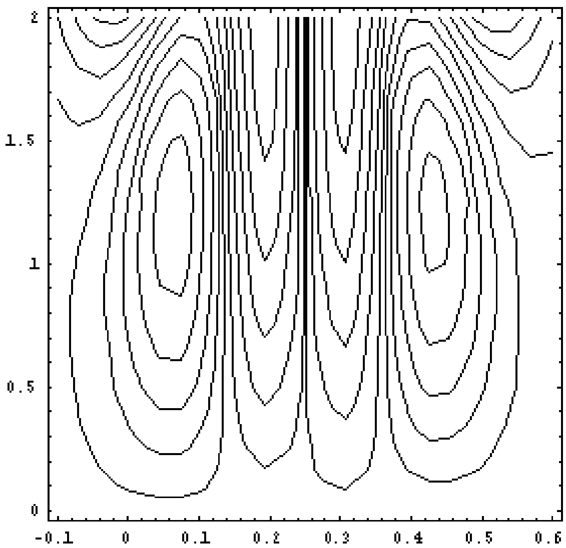

a) E_1 *=1.0 and* E_3 *=0.0*

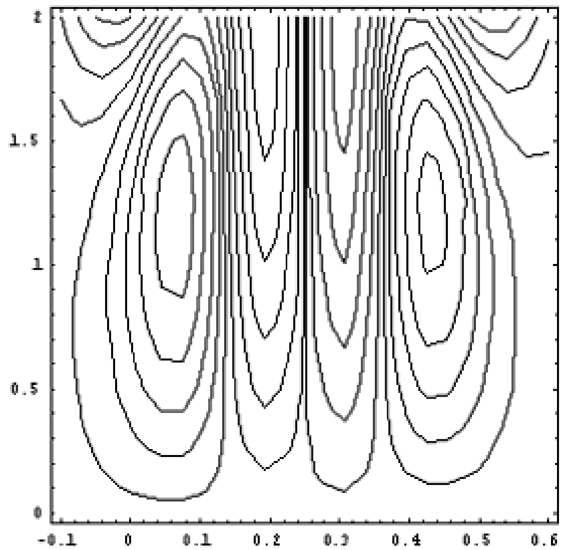

b) E_1 *=1.0 and* E_3 *=0.0*

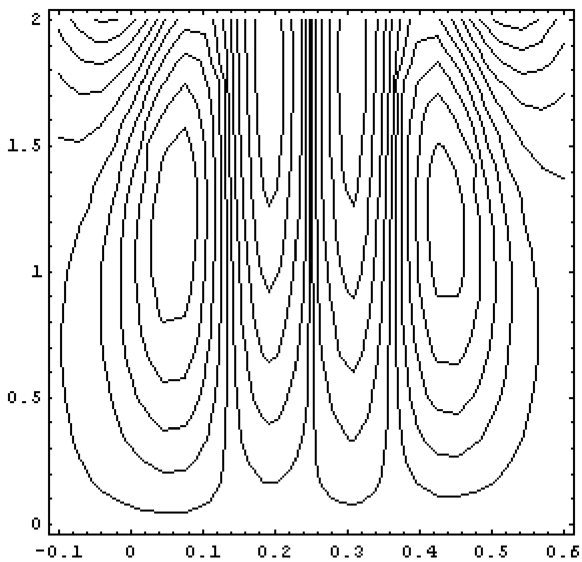

c) E_1 *=1.0 and* E_3 *=0.01*

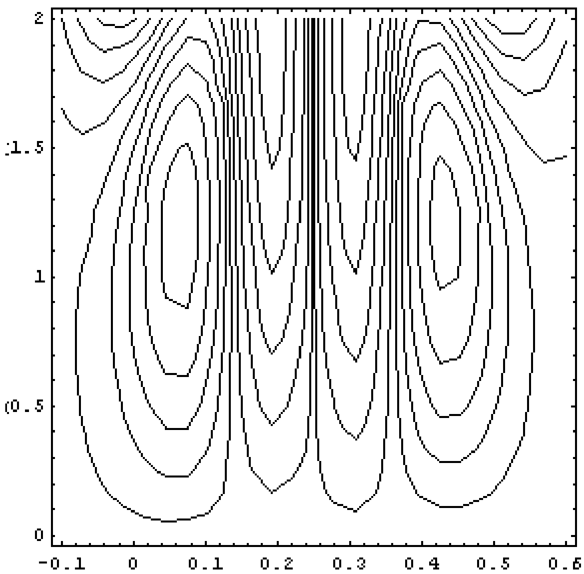

d) E_1 *=1.0 and* E_3 *=0.01*

Figure 2. Effect of E_1 **and** E_3 **on the streamline pattern of fluid particles for** E_2 **=0.2,** δ **=0.2,** $\varepsilon = 0.4$ **M=0.1, R=1 and S=0.5**

Figure 3 shows the effect of the mass characterizing parameter E_2 on the streamline pattern for elastic and dissipative feature of the walls. As the mass concentration parameter E_2 increases, the streamlines get closer and the area of the trapped bolus increases, both for elastic (Figure 3a and b) and dissipative feature of the walls (Figure 3c and 3d). The effect of the mass characterizing parameter (S) on the streamline pattern is shown in Figure 4; change in the character of the streamlines with the variation in the mass concentration of dust particles (S) was not significant. Though trapping was observed and was predominant for all values of S, it can be seen that as the mass concentration of dust particles increased, the area of the trapped bolus in some regions decreased. Figure 5 shows that as we increase the Hartmann, the area of the trapped bolus decreased in some regions. The phenomenon of trapping was observed and the area of the trapped bolus increased along with the tension parameter, but decreased with damping, mass concentration of dust particles and magnetic field.

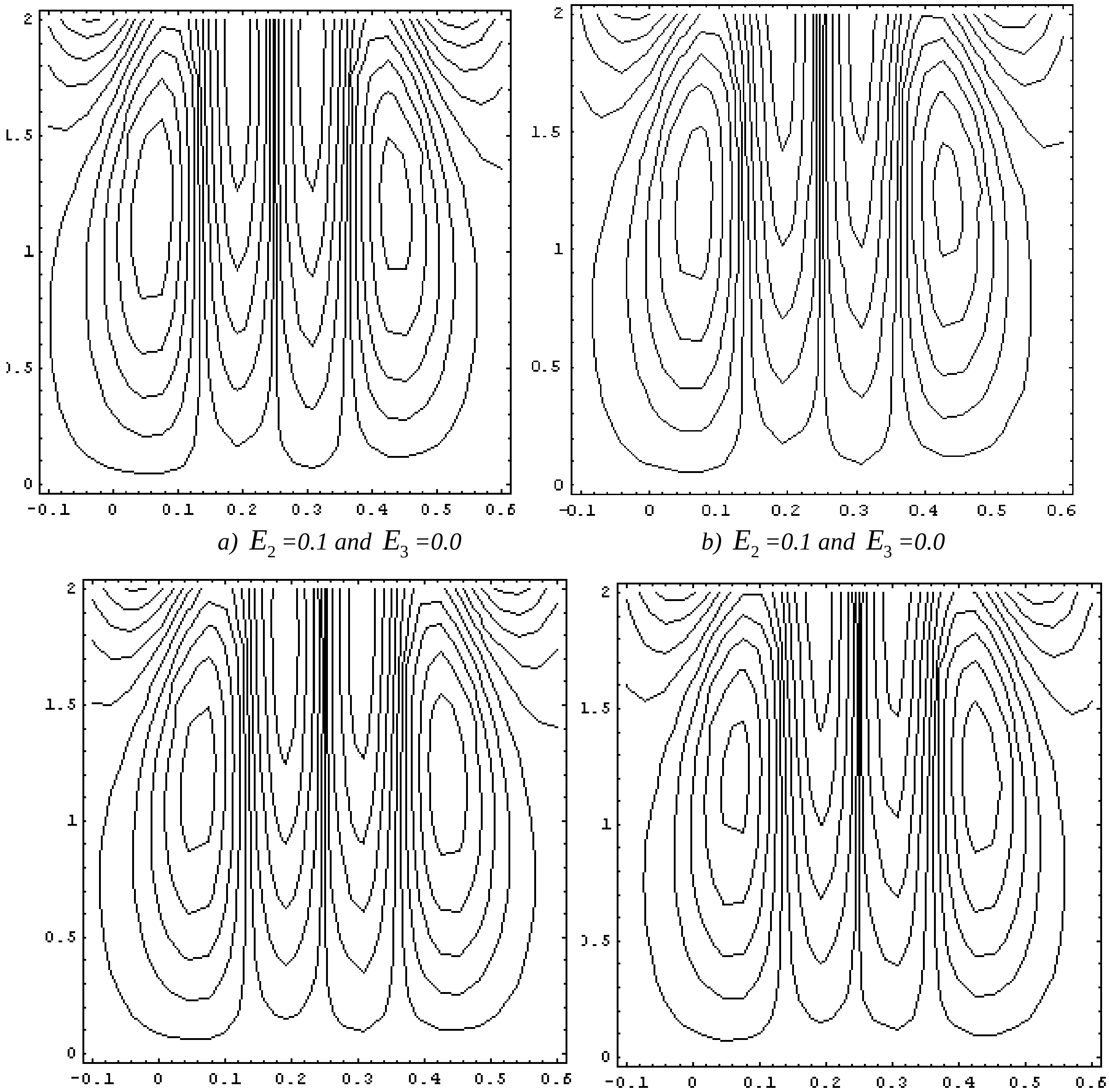

a) E_2 =0.1 and E_3 =0.0   *b) E_2 =0.1 and E_3 =0.0*

c) E_2 =0.1 and E_3 =0.1   *d) E_2 =0.1 and E_3 =0.1*

Figure 3. Effect of E_2 and E_3 on the streamline pattern of fluid particles for E_1 =1.0, δ =0.2, $\varepsilon = 0.4$ M=0.1, R=1 and S=0.5

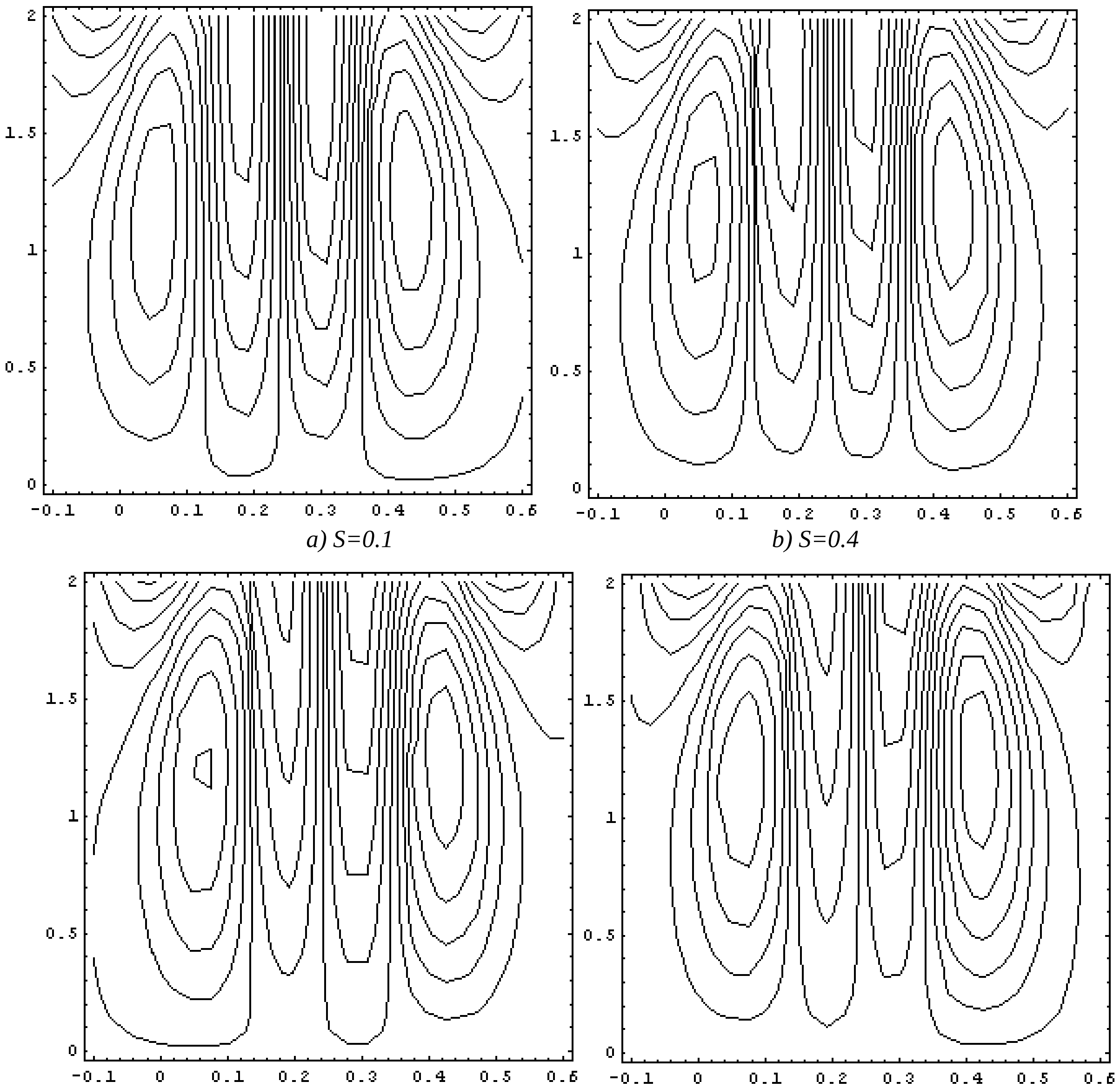

a) S=0.1 *b) S=0.4* *c) S=0.8* *d) S=1.2*

Figure 4. Effect of S on the streamline pattern of fluid particles for E_1 =1.0, E_2 =0.75, E_3 =0.6, δ =0.2, $\varepsilon = 0.4$ M=0.1 and R=1.

The effect of E_1, E_2, E_3, S and M on the average fluid flow rate is shown through the figures 6-10. The phenomenon of reflux, i.e. flow reversal, is observed for all values of the parameter. For higher values of E_1 and E_2, the amplitude ratio at which the fluid flow rate is decreased. It can be seen from Figure 8 that for lower damping values (E_3 =0.2), reflux occurred. Figure 9 shows that for higher mass concentration of dust particles (S=0.8), reflux occurred for amplitude ratio up to 0.2 (approx). Figure 10 shows that for values of the Hartmann number reflux occurred for all values of amplitude ratios.

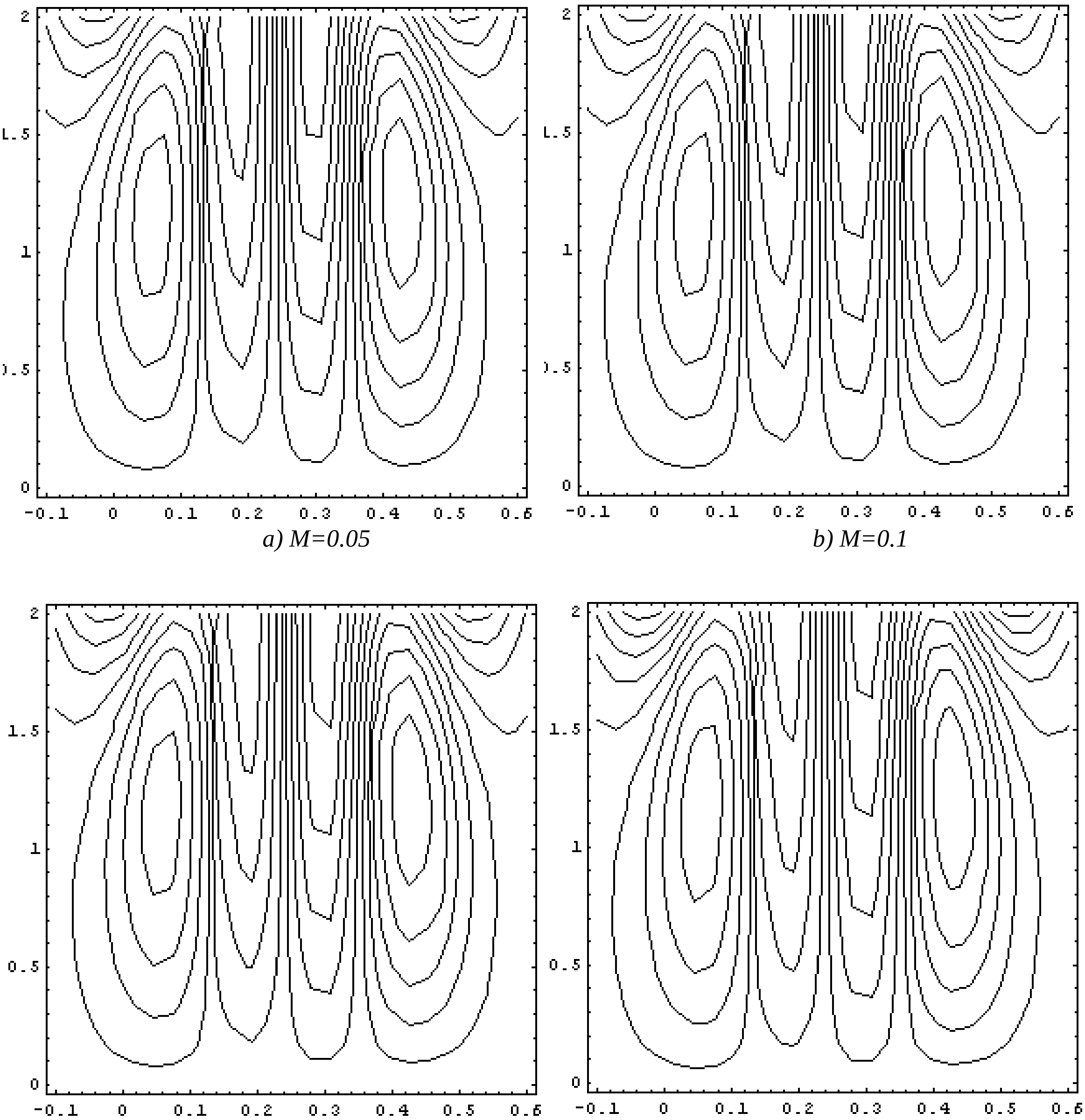

a) M=0.05 *b) M=0.1*

c) M=0.15 *d) M=0.2*

Figure 5. Effect of M on the streamline pattern of fluid particles for E_1 =1.0, E_2 =0.75, E_3 =0.6, δ =0.2, $\varepsilon = 0.4$ S=0.5 and R=1.

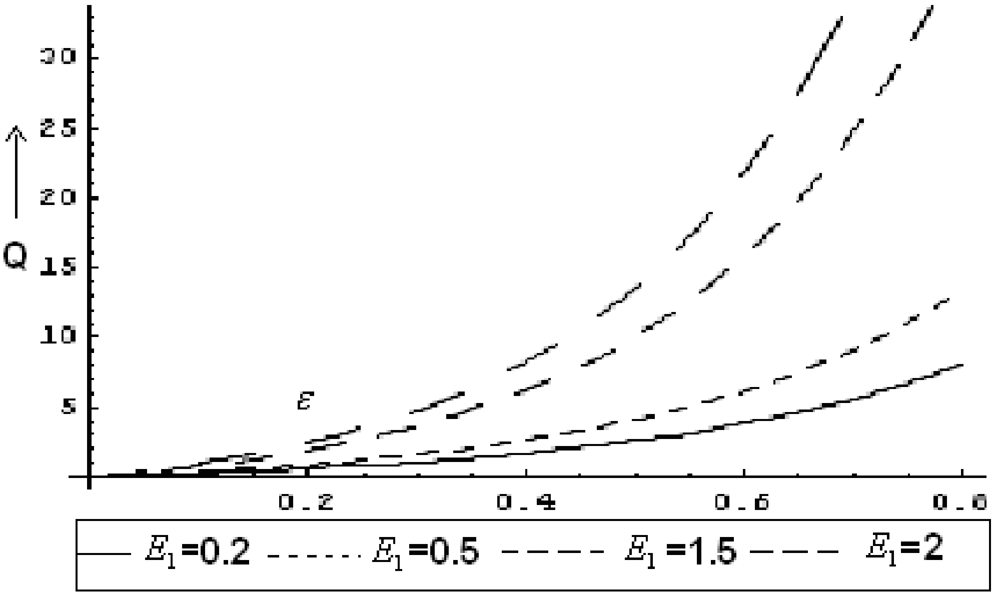

Figure 6: Effect of E_1 on the flow rate of fluid particles for E_2 =0.5, E_3 =0.75, δ =0.1, M=0.1, R=1 and S=0.5.

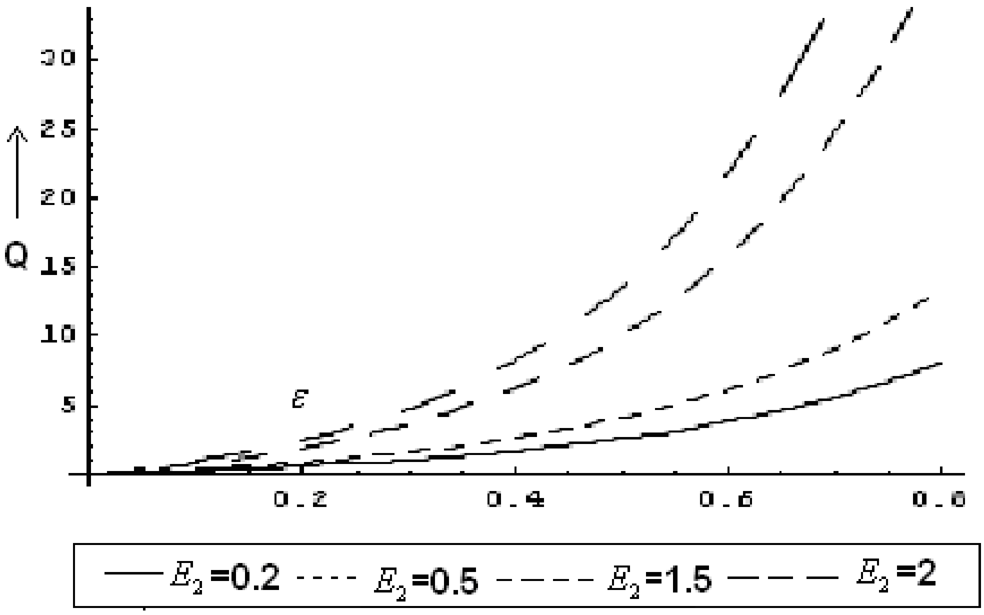

Figure 7: Effect of E_2 on the flow rate of fluid particles for E_1 =0.5, E_3 =0.75, δ =0.1, M=0.1, R=1 and S=0.5

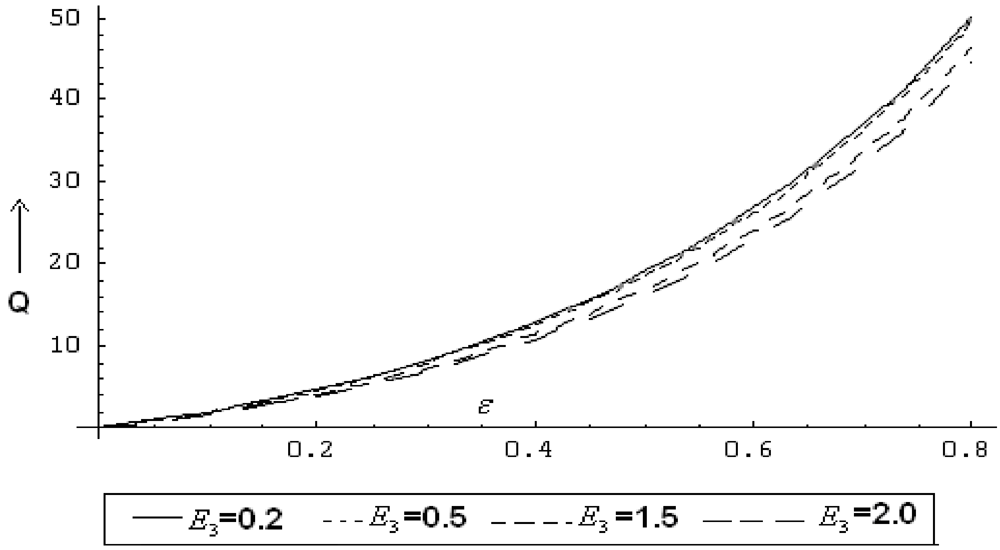

Figure 8: Effect of E_3 on the flow rate of fluid particles for E_1=0.5, E_2 =0.75, δ =0.1, M=0.1, R=1 and S=0.5

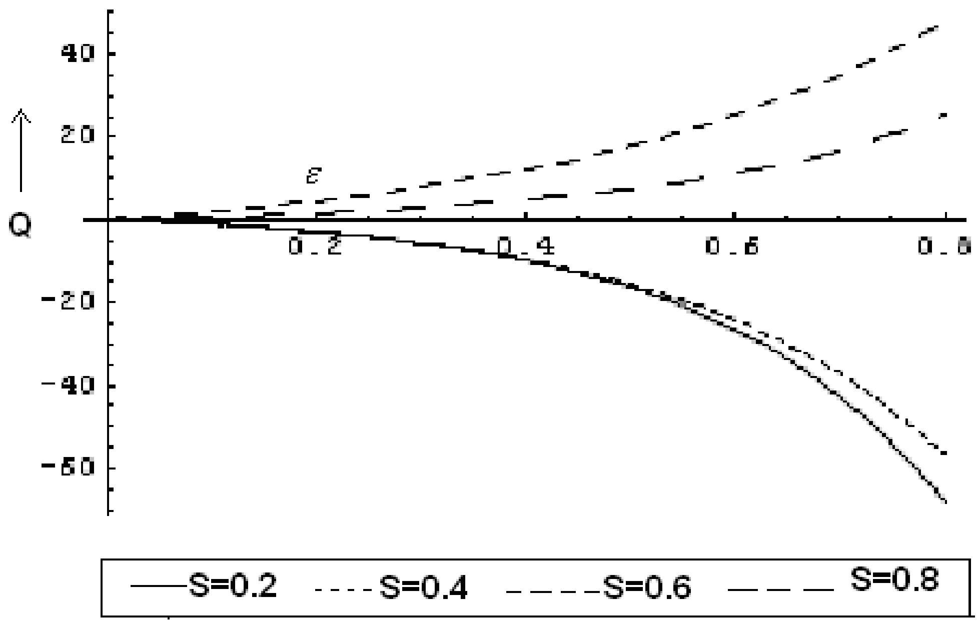

Figure 9: Effect of S on the flow rate of fluid particles for E_1 =0.5, E_2 =0.75, E_3 =0.75, δ =0.1, R=1 and M=0.1.

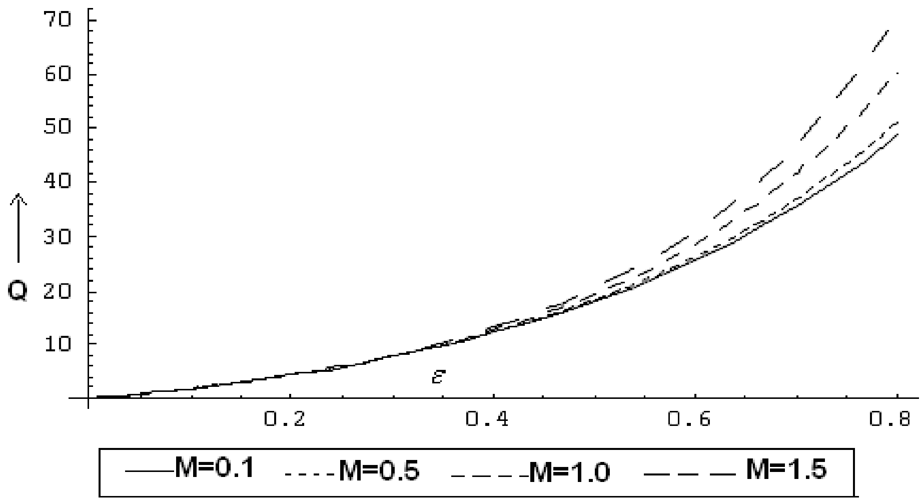

Figure 10: Effect of M on the flow rate of fluid particles for E_1 =0.5, E_2 =0.75, E_3 =0.75, δ =0.1, R=1 and S =0.5.

REFERENCES

[1] Shapiro, A.H., Jaffrin, M.Y., and Weinberg, S.L., *J. Fluid Mech*., 37, 799-825, **1969**.
[2] Fung, Y.C. and Yih, C.S., *J. of Appl. Mech. Trans. ASME*, J. of Appl. Mech. Trans. ASME, 35, 669-675, **1968**.
[3] Jaffrin, M.Y. and Shapiro, A.H., *Ann. Rev. of Fluid Mech*., 3, 13-36, **1971**.
[4] Picologlou, B.F., Patel, P.D., and Lykoudis, P.S., *Biorheol*., 10, 431-440, **1973**.
[5] Srivastava, L.M., *Rheol. Acta*, 25, 638-641, **1986.**
[6] Misery, A.M. Ei., Shehawey, E.F. Ei., and Hakeem, A., *J. Phys. Soc.Japan.* 65, 3524-3529, **1996**.
[7] Srinivasacharya, D., Mishra, M., and Ramachandrarao, A., *Acta. Mech*., 161, 165-178, **2003**.
[8] Saffman, P.G., *J. Fluid Mech*., 13, 120-128, **1962**.
[9] Kaimal, M.R., *J. Appl. Mech., Trans. ASME*, 43, 32-36, **1978**.
[10] Radhakrishnamacharya, G., *ZAMP*, 29, 217-225, **1978**.
[11] Mitra, T.K. and Prasad, S.N., *J. Biomech*., 6, 681-693, **1973**.
[12] Srinivasulu, Ch. and Radhakrishnamacharya, G., *Proc. Nat. Acad. Sci. India*, 72 (A), 279-288, **2002**.
[13] Srinivasacharya, D., Radhakrishnamacharya, G., and Srinivasulu, CH., *Turkish J. Eng. Env. Sci*.32, 357-365, **2008**.
[14] Rathod,V.P and Asha.S.K, *Journal of Ultra Science* 21, **2009**, .83-90.
[15] Rathod, V.P and Mahadev, M., *Journal of Ultra Science*, **2011**, accepted.